Impact of the Southern Annular Mode on the seasonal cycle of Antarctic sea ice extent

Edward W. Doddridge[1] **and John Marshall**[1]

[1]Earth, Atmospheric and Planetary Science, Massachusetts Institute of Technology, 77 Massachusetts Avenue, Cambridge, 02139, USA

Key Points:

- Southern Annular Mode anomalies are correlated with a detectable change in the seasonal cycle of sea ice extent
- Positive values of the summertime Southern Annular Mode lead to increased sea ice extent during the following autumn
- Recent record minimum in sea ice extent is partially explained by the negative SAM during 2016/17 austral summer

Corresponding author: Edward W. Doddridge, `ewd@mit.edu`

Abstract

Through analysis of remotely-sensed sea surface temperature (SST) and sea ice concentration data we investigate the impact of the Southern Annular Mode (SAM) on sea ice extent around Antarctica. We show that positive SAM anomalies in the austral summer produce anomalously cold SSTs that persist and lead to anomalous ice growth in the following autumn, while negative SAM anomalies lead to a reduction in sea ice extent during autumn. The imprint of SAM appears to be seasonal: SST and ice extent anomalies do not persist from one year to the next, rather the system resets itself each winter. Our analysis shows the recent record minimum in Antarctic sea ice extent is likely associated with the strongly negative SAM during the 2016/17 austral summer.

1 Introduction

The Southern Annular Mode (SAM) is the dominant mode of variability in the extratropical Southern Hemisphere [*Gong and Wang*, 1999; *Thompson and Wallace*, 2000]. The SAM is the leading empirical orthogonal function in a number of variables: geopotential height; surface temperature; surface pressure; and zonal winds [*Thompson and Wallace*, 2000]. Positive SAM anomalies are associated with a strengthening and a poleward shift of the midlatitude westerlies over the Southern Ocean [*Thompson and Wallace*, 2000]. The observational record shows a statistically significant increase in SAM over the most recent decades [*Marshall*, 2003]. There is a seasonal bias to this increase; the effect is largest in the austral summer (December, January, and February). This seasonality is likely linked to the depletion of stratospheric ozone over Antarctica [*Polvani et al.*, 2011]. The seasonal SAM index from 1970 is shown in figure 1 a) along with the trend line for the summertime SAM.

The anomalous westerly winds over the Southern Ocean associated with SAM perturbations lead to anomalies in the sea surface temperature (SST). These temperature anomalies are largely caused by additional Ekman transport in the upper ocean [*Ferreira et al.*, 2015; *Purich et al.*, 2016], but atmospheric feedbacks also play an important role [*Seviour et al.*, 2016, 2017]. The anomalous Ekman transports converge or diverge at approximately 55 S for positive and negative SAM anomalies respectively [*Kostov et al.*, 2016]. During positive SAM anomalies, the upper ocean south of the convergence is cooled by the transport of cold water northwards; north of the convergence the SST is warmed. The anomalous January winds associated with a $+1\sigma$ summertime SAM are shown in figure 1 b).

Recent reviews have clearly articulated the complexity of the ocean-ice-atmosphere system in the Southern Hemisphere, and demonstrated that a detailed understanding of this complex system does not yet exist [*Hobbs et al.*, 2016; *Jones et al.*, 2016]. Large-scale observation of Southern Hemisphere sea ice has only been possible since the advent of the satellite era at the end of the 1970s. During this time there has been a statistically significant increase in sea ice extent, dominated by the positive trend in the Western Ross Sea [*Hobbs et al.*, 2016]. It has been suggested that the substantial internal variability in the observational record will mask the forced response for several decades [*Goosse et al.*, 2009; *Jones et al.*, 2016]. As well as substantial interannual variability, the Southern Ocean undergoes an extensive seasonal cycle: each year approximately 15 million square kilometers of ice forms and subsequently melts. The climatology and variability of sea ice in the Southern Ocean are shown in figure 1 c).

The regional response of sea ice to the SAM has been explored, with some studies showing clear patterns of regionality in sea ice anomalies associated with SAM perturbations [*Liu et al.*, 2004; *Simpkins et al.*, 2012]. Other studies have suggested that local winds, which may not be related to the SAM, are more important [*Holland and Kwok*, 2012]. The difficulties associated with using an annular mode to explain hemispheric sea ice extent changes are exemplified by the record sea ice extents in 2012, 2013, and 2014, which exhibited marked differences in the locations of the sea ice anomalies [*Reid and Massom*, 2015]. *Kohyama and Hartmann* [2016] explore correlations between modes of atmospheric variability, including

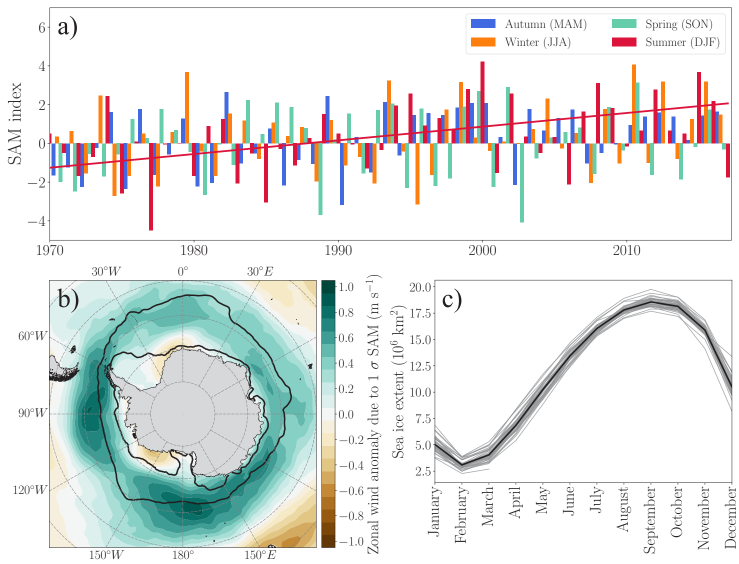

Figure 1. The Southern Annular Mode (SAM) and sea ice. a) the observational record of the SAM in each season from 1970 and the trend line for DJF SAM [*Marshall*, 2003], b) the zonal wind anomaly in January associated with a $+1\sigma$ DJF SAM from ERA-Interim reanalysis winds [*Dee et al.*, 2011] (colors) along with the 15% sea ice concentration contour during the months of minimum (February) and maximum (September) sea ice extent from satellite data [*Reynolds et al.*, 2002], and c) the seasonal cycle in sea ice extent, defined as the area covered by ice with a concentration of at least 15%, with individual years shown in gray and the climatology in black [*Fetterer et al.*, 2016].

the SAM, and variations in sea ice. They find some evidence of the SAM affecting Antarctic sea ice in the Indian Ocean sector during May, June, and July, but conclude that sea ice extent is not well explained by the contemporaneous SAM index.

The equilibrium response of sea ice extent to changes in the SAM has been studied using coupled general circulation models, which suggest that an increase in the SAM will lead to a decrease in sea ice extent [*Sigmond and Fyfe*, 2010, 2013]. The link between SAM and SIE is complicated by the observational record, which shows several decades of increasing SAM [*Marshall*, 2003] concurrent with an increase in sea ice extent [*Zwally et al.*, 2002]. However, there have been multiple years of record sea ice extent in the past decade [*Reid and Massom*, 2015], during which there has been no appreciable trend in the SAM [*Jones et al.*, 2016]. Multiple studies have found no evidence of a link between the long term trends in SAM and SIE [*Kohyama and Hartmann*, 2016; *Lefebvre et al.*, 2004; *Simpkins et al.*, 2012]. *Ferreira et al.* [2015] propose a two timescale response as a solution to this dichotomy; over "short" timescales an increase in SAM drives an increase in sea ice extent by cooling the sea surface, while eventual upwelling of warmer circumpolar deep water leads to a decrease in sea ice extent over longer timescales [*Ferreira et al.*, 2015; *Holland et al.*, 2016; *Kostov et al.*, 2016].

In this paper we use composites and regression analysis to explore the seasonal response of the Southern Ocean to SAM anomalies during the austral summer. Despite the difficulties described previously, and the complexity of the system, we show a robust signal consistent with a simple, physically motivated mechanism. The paper is structured as follows. First we explore the SST response to SAM anomalies, then we calculate the effect on sea ice concentration. Following this we examine the changes in sea ice extent driven by summertime SAM anomalies. In the final section we discuss several individual years and show that this mechanism likely contributed to the negative sea ice extent anomaly observed in early 2017.

2 Response to summertime SAM anomalies

We consider the seasonal impact of SAM anomalies by examining the response of the Southern Ocean using a range of observational data products. These products are: an observational SAM index that begins in 1957 [*Marshall*, 2003], satellite derived sea surface temperatures and sea ice concentration from December 1981 onwards [*Reynolds et al.*, 2002], and sea ice extent for the Southern Hemisphere from October 1978 [*Fetterer et al.*, 2016]. The seasonal impact of SAM on sea surface temperature and sea ice is assessed using composites and linear regression.

The summertime SAM time series, defined as the average SAM value during December, January and February, is detrended by performing a linear regression and subtracting the linear fit from the data. This gives a time series with a mean of zero and no linear slope. Following *Marshall* [2003] the year associated with each summertime SAM is the year in which the December occurred. The SST and sea ice concentration data are detrended at each grid point using the same method. The SIE time series is also detrended by removing the linear fit from the data.

The positive SAM composites are constructed by combining years following detrended summertime SAMs larger than 1, while the negative composites combine all years following detrended summertime SAMs less than -1. The negative SAM SST and sea ice concentration composites contain data from 9 years (1983, 1985, 1987, 1992, 2001, 2004, 2006, 2010, and 2017) and the positive composites contain data from 10 years (1982, 1989, 1994, 1995, 1999, 2000, 2002, 2008, 2012, and 2015). Because the sea ice extent record is longer than the other data sets, it begins in late 1978, the sea ice extent composites each contain an additional year; the negative SAM sea ice extent composite contains data from 1980, and the positive SAM composite contains data from 1981. We also analyze sea ice extent with a regression analysis, in which we regress the detrended summertime SAM time series against the detrended monthly sea ice extent data for each calendar month. Thus, the regression slope for each month describes the change in sea ice extent expected from a unit change in the detrended summertime SAM.

In the supplementary information we present the results of several additional analyses: composite analysis of the raw SST and sea ice concentration data, and regression analysis applied to both raw and detrended SST and sea ice concentration data. This ensures that our results are not due to any long-term covariability between the variables.

2.1 Sea surface temperature response to summertime SAM

We use the SST composites constructed from the detrended dataset to examine the effect of the summertime SAM on SST around Antarctica. In the supplementary information we show results from a composite analysis using the raw datasets as well as a regression analysis applied to both the raw and detrended datasets.

Positive SAM anomalies during the austral summer months of December, January, and February (DJF) are associated with anomalously strong westerly winds. These wind anomalies cause a cooling of the sea surface surrounding Antarctica and warming farther north largely driven by anomalous meridional Ekman transports [*Ferreira et al.*, 2015; *Kostov et al.*, 2016; *Purich et al.*, 2016]. Assuming that the thickness of the Ekman layer is equal to or smaller than the depth of the mixed layer, we expect the temporal evolution of the zonal mean SST anomaly, $\langle SST \rangle'$, to be given by

$$\frac{\partial \langle SST \rangle'}{\partial t} = \frac{\tau_x'}{\rho_0 f h} \frac{\partial \overline{\langle SST \rangle}}{\partial y} - \lambda \langle SST \rangle' \qquad (1)$$

where $\langle SST \rangle'$ is the anomaly in zonal mean sea surface temperature, τ_x' is the anomalous zonal wind forcing, ρ_0 is the reference density, f is the Coriolis parameter, h is the mixed layer depth, $\partial\overline{\langle SST \rangle}/\partial y$ is the meridional derivative of the zonally averaged climatological sea surface temperature, and $1/\lambda$ is the relaxation timescale associated with damping of SST anomalies. In the absence of damping, the magnitude of the expected response is proportional to the meridional SST gradient, and inversely proportional to the mixed layer depth. We use equation (1) as a simple model to understand the temporal evolution of these SST anomalies.

Maps of the SST anomalies from our composite analysis can be seen in figure 2 a) and b). The temporal evolution of these SST anomalies can be more clearly studied by calculating the mean SST anomaly between 50 S and 70 S from our detrended composites and examining its variation with time. This allows us to examine the magnitude of the initial perturbation and the decay time scale of the induced temperature anomalies. The integrated SST anomalies are shown in figure 3 a) as a function of time (note that the negative SAM composite has been multiplied by -1 to aid comparisons between the composites). The integrated SST anomalies differ at a statistically significant level in January ($p \approx 0.017$), February ($p \approx 0.0012$), March ($p \approx 0.019$), and April ($p \approx 0.023$). After May ($p \approx 0.057$) the difference between the composites is not statistically significant using Welch's unequal variances t-test.

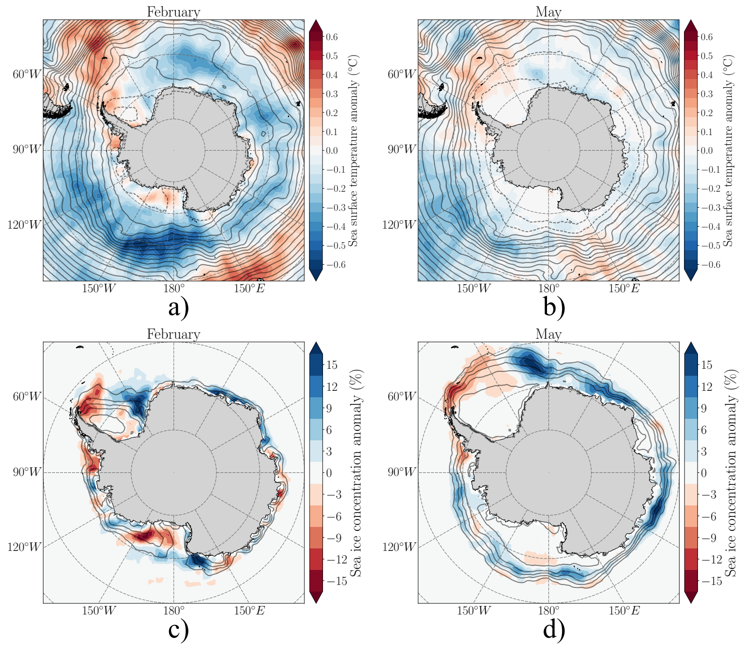

Figure 2. Maps of sea surface temperate and sea ice concentration changes in response to DJF SAM anomalies, calculated as the positive composite minus the negative composite, divided by two. SST anomalies in February (a) and May (b), and sea ice concentration anomalies in February (c) and May (d). The colors show the anomalies while the contours show the climatology. The SST contours are at 0.5±1.0, 2.0,...°C with the negative contours dashed, while the sea ice concentration contours are at 10%, 30%, 50%, 70%, and 90%.

SST anomalies are damped by both atmospheric and oceanic processes. The damping timescale for SST anomalies depends on their latitude and horizontal extent, as well as

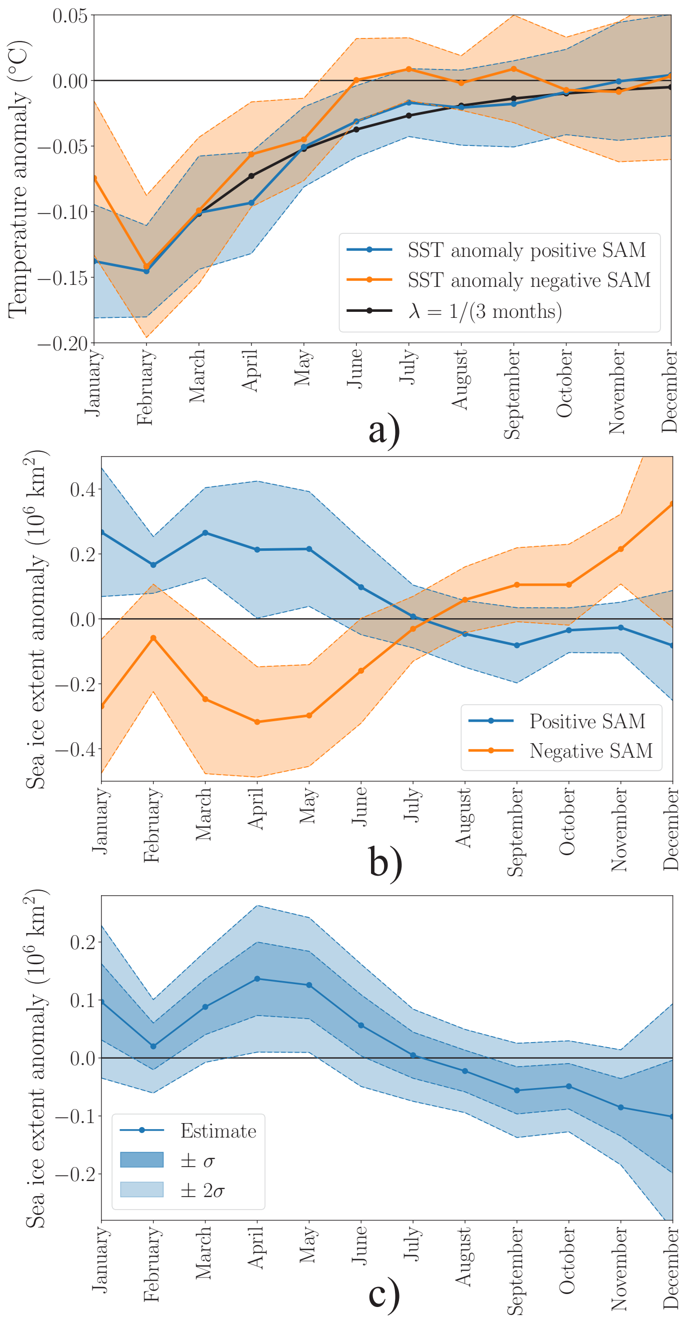

Figure 3. Integrated response of sea surface temperature and sea ice to DJF SAM anomalies. a) mean temperature anomaly between 50 S and 70 S for the positive and negative SAM composites, b) evolution of SIE anomaly from the composites, and c) computed using regression analysis. In a), the SST values from the negative SAM composite have been multiplied by -1 to make comparisons easier and the black curve shows an exponential decay with a timescale of three months. The sea ice extent composites, shown in b), are significantly different in May ($p < 0.05$), while the regression analysis, shown in c), suggests that the effect is significant in both April and May ($p < 0.05$).

the season [*Hausmann et al.*, 2016]. Of the oceanic processes, the most important is the entrainment of fluid from below the mixed layer as the mixed layer deepens; hence the seasonal dependency in the damping timescale. Consistent with previous studies that have estimated a damping timescale of 3-6 months for large-scale temperature anomalies in the Southern Ocean during the austral autumn [*Ciasto and Thompson*, 2008; *Hausmann et al.*, 2016], we find a damping timescale of approximately 2.5 - 3 months (see supplementary information). This suggests that SST anomalies may persist for long enough to affect the seasonal cycle of sea ice growth.

2.2 Sea ice response to summertime SAM anomalies

We expect the SAM induced SST anomalies to cause changes in the sea ice concentration, with warmer SSTs reducing ice cover and colder SSTs promoting ice. Our analysis shows that autumns following positive DJF SAM anomalies tend to have more sea ice, while autumns following negative DJF SAM anomalies generally have less sea ice. The sea ice concentration changes computed from the detrended composites are shown in figure 2 c) and d).

Changes to the sea ice extent, which is calculated as the area covered by sea ice with a concentration of at least 15%, depend not only on changes in concentration, but also on the background state. If there are large areas of ice near this threshold, then small changes in concentration can lead to large changes in extent. Conversely, if the area of sea ice near the 15% cut-off is small, then the change in sea ice extent will also be small. The large year-to-year variation in the spatial distribution of sea ice has complicated previous attempts to explain the impact of SAM anomalies on sea ice extent [*Reid and Massom*, 2015]. Here we sidestep this issue by focusing on the zonally integrated response of sea ice to SAM anomalies, rather than the regional response.

Following DJF SAM anomalies we find a signal in sea ice extent that persists for many months, as shown in figure 3 b) and c). In figure 3 b) the shaded regions show the standard error of the mean, given by the standard deviation of the composite divided by the square root of the number of composite members (11 for positive SAM, 9 for negative SAM). The difference between the two composites is statistically significant in May ($p \approx 0.043$). In figure 3 c) the error estimate, σ, is computed as the uncertainty in the regression slope for each month. The regression slope is statistically distinguishable from zero in April ($p \approx 0.039$) and May ($p \approx 0.038$). The results in figure 3 b) and c) show that following positive SAM anomalies sea ice extent is increased relative to the climatology, while negative SAM anomalies cause a decrease in sea ice extent. The magnitude of this perturbation reaches a maximum in April and May, before decreasing. The fading of these signals over winter is consistent with the assertion that the long-term impact of SAM on sea ice extent is due to subsurface dynamics [*Ferreira et al.*, 2015]. Our finding that the system resets over winter is also consistent with previous work analyzing the timing of the onset of freezing and thawing in the Southern Ocean [*Stammerjohn et al.*, 2012].

3 Individual years

Figure 4 shows detrended sea ice extent anomalies for all years following a detrended DJF SAM greater than 1 or less than -1. Despite the large amount of variability, there is a clear trend for years following positive SAMs to have more ice, and years following negative SAMs to have less ice, especially during April and May. In particular, the largest positive sea ice extent anomalies occurred following large positive SAM anomalies. The sea ice extent curves for four individual years have been labeled. These years correspond to the most extreme January sea ice extent anomalies. The SAM values are as expected: positive for the positive sea ice extent anomalies, and negative for the negative sea ice extent anomalies.

The detrended summertime SAM in 2016/17 was a remarkable -3.4, resulting in anomalously cold SSTs across the Southern Ocean. Based on our regression analysis, we expect

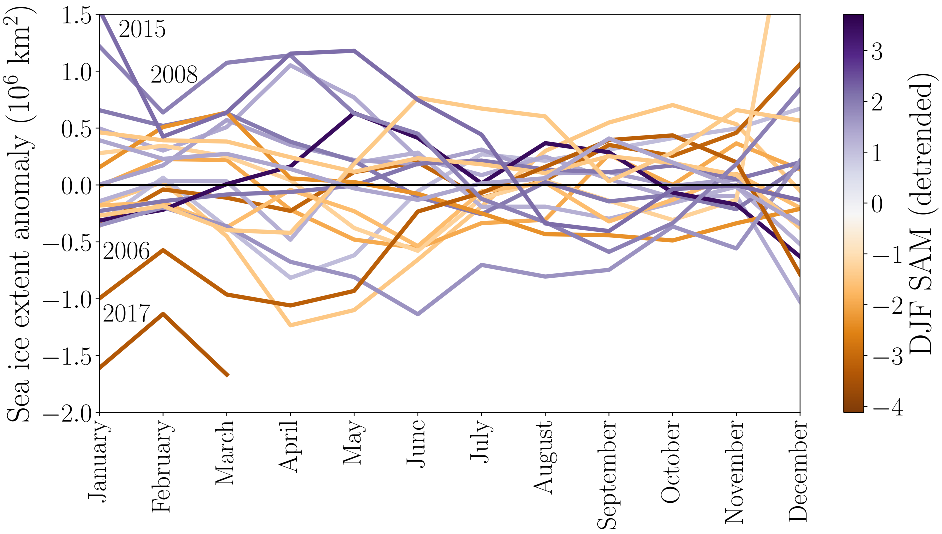

Figure 4. The temporal evolution of detrended sea ice extent anomaly for years following detrended DJF SAM values greater than 1 or less than -1. The two years with very positive sea ice extent anomalies are 2015, following a DJF SAM of 2.4, and 2008, following a DJF SAM of 2.1. The most negative January anomaly is 2017, following a DJF SAM of -3.4, and 2006, following a DJF SAM of -3.0.

this to cause a sea ice extent anomaly of just over -0.3×10^6 km^2 in March. The observed anomaly is closer to -1.5×10^6 km^2 which means our mechanism cannot fully explain the observed anomaly. In addition to the negative DJF SAM, the SAM was strongly negative in November 2016. It is likely that this negative November SAM also contributed to the observed record low sea ice extent through the same mechanism we have discussed for the DJF SAM. Our study suggests that the impact of the negative DJF SAM will likely dissipate by August as the mixed layer deepens, mixing away the cold SST imprint of the SAM: note how the curves in figure 4 converge by October. Therefore we expect the SIE anomaly to decrease as we approach the maximum ice extent in September.

4 Conclusions

We have used observational data to investigate the impact of DJF SAM anomalies on sea surface temperature and sea ice extent during the following year. Our analysis of SST anomalies corroborates earlier results suggesting that the damping timescale for hemispheric SST anomalies near Antarctica is between three and six months [*Ciasto and Thompson*, 2008; *Hausmann et al.*, 2016], and suggests that it may be closer to three months. Consistent with previous studies we find that anomalies in the SST lead to anomalies in sea ice concentration [*Fan et al.*, 2014].

We find that the seasonal response of sea ice extent to DJF SAM anomalies is consistent regardless of whether we use regression or composites to analyze the data. The signal is also present in both the raw and the detrended datasets. This provides strong evidence that our results are due to seasonal effects and not long-term covariability between the SAM and sea ice extent. Positive SAM anomalies lead to anomalously cold SST around Antarctica, and an expansion of sea ice. Negative SAM anomalies produce the opposite response, with warmer SST around Antarctica and a reduction in sea ice extent. In both cases the magnitude of the sea ice extent anomaly reaches a maximum in the autumn and decays by the end of winter. This finding suggests that the current sea ice extent anomaly will decrease in magnitude as the ice growth season continues. The relationship between the summertime SAM and sea ice extent has implications for the seasonal prediction of sea ice extent in future years.

Acknowledgments
We gratefully acknowledge Dave Thompson for his advice, and two anonymous reviewers whose input greatly improved this manuscript. This study was supported by a US National Science Foundation grant of the NSF Antarctic Program.

The data that support the findings in this study can be accessed in the following locations:

The observational SAM index was downloaded from http://www.nerc-bas.ac.uk/icd/gjma/sam.html

NOAA_OI_SST_V2 data provided by the NOAA/OAR/ESRL PSD, Boulder, Colorado, USA, from their web site at http://www.esrl.noaa.gov/psd/

The sea ice extent time series, Sea Ice Index V2, was downloaded from the National Snow & Ice Data Center, at ftp://sidads.colorado.edu/DATASETS/NOAA/G02135/south/daily/data/

ERA-Interim reanalysis winds were obtained from http://apps.ecmwf.int/datasets/data/interim-full-moda/levtype=sfc/

References

Ciasto, L. M., and D. W. J. Thompson (2008), Observations of large-scale ocean-atmosphere interaction in the Southern Hemisphere, *J. Clim.*, *21*(6), 1244–1259, doi:10.1175/2007JCLI1809.1.

Dee, D. P., S. M. Uppala, A. J. Simmons, P. Berrisford, P. Poli, S. Kobayashi, U. Andrae, M. A. Balmaseda, G. Balsamo, P. Bauer, P. Bechtold, A. C. M. Beljaars, L. van de Berg, J. Bidlot, N. Bormann, C. Delsol, R. Dragani, M. Fuentes, A. J. Geer, L. Haimberger, S. B. Healy, H. Hersbach, E. V. Hólm, L. Isaksen, P. Kållberg, M. Köhler, M. Matricardi, A. P. McNally, B. M. Monge-Sanz, J.-J. Morcrette, B.-K. Park, C. Peubey, P. de Rosnay, C. Tavolato, J.-N. Thépaut, and F. Vitart (2011), The ERA-Interim reanalysis: configuration and performance of the data assimilation system, *Q. J. R. Meteorol. Soc.*, *137*(656), 553–597, doi:10.1002/qj.828.

Fan, T., C. Deser, and D. Schneider (2014), Recent sea ice trend in the context of Southern Ocean surface climate variations since 1950, *Geophys. Res. Lett.*, pp. 2419–2426, doi:10.1002/2014GL059239.Received.

Ferreira, D., J. Marshall, C. M. Bitz, S. Solomon, and A. Plumb (2015), Antarctic ocean and sea ice response to ozone depletion: A two-time-scale problem, *J. Clim.*, *28*(3), 1206–1226, doi:10.1175/JCLI-D-14-00313.1.

Fetterer, F., K. Knowles, W. Meier, M. Savoie, and A. K. Windnagel (2016), Sea Ice Index, Version 2 [Southern Hemisphere], doi:10.7265/N5736NV7.

Gong, D., and S. Wang (1999), Definition of Antarctic Oscillation index, *Geophys. Res. Lett.*, *26*(4), 459–462, doi:10.1029/1999GL900003.

Goosse, H., W. Lefebvre, A. de Montety, E. Crespin, and A. H. Orsi (2009), Consistent past half-century trends in the atmosphere, the sea ice and the ocean at high southern latitudes, *Clim. Dyn.*, *33*(7-8), 999–1016, doi:10.1007/s00382-008-0500-9.

Hausmann, U., A. Czaja, and J. Marshall (2016), Estimates of AirâĂŞSea Feedbacks on Sea Surface Temperature Anomalies in the Southern Ocean, *J. Clim.*, *29*(2), 439–454, doi:10.1175/JCLI-D-15-0015.1.

Hobbs, W. R., R. Massom, S. Stammerjohn, P. Reid, G. Williams, and W. Meier (2016), A review of recent changes in Southern Ocean sea ice, their drivers and forcings, *Glob. Planet. Change*, *143*, 228–250, doi:10.1016/j.gloplacha.2016.06.008.

Holland, M. M., L. Landrum, Y. Kostov, and J. Marshall (2016), Sensitivity of Antarctic sea ice to the Southern Annular Mode in coupled climate models, *Clim. Dyn.*, pp. 1–19, doi:10.1007/s00382-016-3424-9.

Holland, P. R., and R. Kwok (2012), Wind-driven trends in Antarctic sea-ice drift, *Nat. Geosci.*, *5*(12), 872–875, doi:10.1038/ngeo1627.

Jones, J. M., S. T. Gille, H. Goosse, N. J. Abram, P. O. Canziani, D. J. Charman, K. R. Clem, X. Crosta, C. de Lavergne, I. Eisenman, M. H. England, R. L. Fogt, L. M. Frankcombe, G. J. Marshall, V. Masson-Delmotte, A. K. Morrison, A. J. Orsi, M. N. Raphael, J. A. Renwick, D. P. Schneider, G. R. Simpkins, E. J. Steig, B. Stenni, D. Swingedouw, and T. R. Vance (2016), Assessing recent trends in high-latitude Southern Hemisphere surface climate, *Nat. Clim. Chang.*, *6*(10), 917–926, doi:10.1038/nclimate3103.

Kohyama, T., and D. L. Hartmann (2016), Antarctic sea ice response to weather and climate modes of variability, *J. Clim.*, *29*(2), 721–741, doi:10.1175/JCLI-D-15-0301.1.

Kostov, Y., J. Marshall, U. Hausmann, K. C. Armour, D. Ferreira, and M. M. Holland (2016), Fast and slow responses of Southern Ocean sea surface temperature to SAM in coupled climate models, *Clim. Dyn.*, pp. 1–15, doi:10.1007/s00382-016-3162-z.

Lefebvre, W., H. Goosse, R. Timmermann, and T. Fichefet (2004), Influence of the Southern Annular Mode on the sea ice - Ocean system, *J. Geophys. Res. C Ocean.*, *109*(9), 1–12, doi:10.1029/2004JC002403.

Liu, J., J. A. Curry, and D. G. Martinson (2004), Interpretation of recent Antarctic sea ice variability, *Geophys. Res. Lett.*, *31*(2), 2000–2003, doi:10.1029/2003GL018732.

Marshall, G. J. (2003), Trends in the Southern Annular Mode from Observations and Reanalyses, *J. Clim.*, *16*, 4134–4143, doi:10.1175/1520-0442(2003)016<4134:TITSAM>2.0.CO;2.

Polvani, L. M., D. W. Waugh, G. J. P. Correa, and S. W. Son (2011), Stratospheric Ozone Depletion: The Main Driver of Twentieth-Century Atmospheric Circulation Changes in the Southern Hemisphere, *J. Clim.*, *24*(3), 795–812, doi:Doi 10.1175/2010jcli3772.1.

Purich, A., W. Cai, M. H. England, and T. Cowan (2016), Evidence for link between modelled trends in Antarctic sea ice and underestimated westerly wind changes., *Nat. Commun.*, *7*(May 2015), 10,409, doi:10.1038/ncomms10409.

Reid, P., and R. A. Massom (2015), Successive Antarctic sea ice extent records during 2012, 2013, and 2014, in *State Clim. 2014*, edited by J. Blunden and D. S. Arndt, pp. S163–S164, American Meteorological Society, doi:10.1175/2015BAMSStateoftheClimate.1.

Reynolds, R. W., N. A. Rayner, T. M. Smith, D. C. Stokes, and W. Wang (2002), An improved in situ and satellite SST analysis for climate, *J. Clim.*, *15*(13), 1609–1625, doi:10.1175/1520-0442(2002)015<1609:AIISAS>2.0.CO;2.

Seviour, W. J., A. Gnanadesikan, D. Waugh, and M. A. Pradal (2017), Transient response of the Southern Ocean to changing ozone: Regional responses and physical mechanisms, *J. Clim.*, *30*(7), 2463–2480, doi:10.1175/JCLI-D-16-0474.1.

Seviour, W. J. M., A. Gnanadesikan, and D. W. Waugh (2016), The Transient Response of the Southern Ocean to Stratospheric Ozone Depletion, *J. Clim.*, *29*(20), 7383–7396, doi:10.1175/JCLI-D-16-0198.1.

Sigmond, M., and J. C. Fyfe (2010), Has the ozone hole contributed to increased Antarctic sea ice extent?, *Geophys. Res. Lett.*, *37*(18), doi:10.1029/2010GL044301.

Sigmond, M., and J. C. Fyfe (2013), The Antarctic Sea Ice Response to the Ozone Hole in Climate Models, *J. Clim.*, *27*, 1336–1342, doi:10.1175/JCLI-D-13-00590.1.

Simpkins, G. R., L. M. Ciasto, D. W. J. Thompson, and M. H. England (2012), Seasonal relationships between large-scale climate variability and antarctic sea ice concentration, *J. Clim.*, *25*(16), 5451–5469, doi:10.1175/JCLI-D-11-00367.1.

Stammerjohn, S., R. Massom, D. Rind, and D. Martinson (2012), Regions of rapid sea ice change: An inter-hemispheric seasonal comparison, *Geophys. Res. Lett.*, *39*(6), 1–8, doi:10.1029/2012GL050874.

Thompson, D. W. J., and J. M. Wallace (2000), Annular Modes in the Extratropical Circulation. Part I: Month-to-Month Variability*, *J. Clim.*, *13*(5), 1000–1016, doi:10.1175/1520-

0442(2000)013<1000:AMITEC>2.0.CO;2.

Zwally, H. J., J. C. Comiso, C. L. Parkinson, D. J. Cavalieri, and P. Gloersen (2002), Variability of Antarctic sea ice 1979-1998, *J. Geophys. Res.*, *107*(C5), 3041–3059, doi: 10.1029/2000JC000733.